



**INTERNATIONAL JOURNAL OF ENGINEERING SCIENCES & RESEARCH  
TECHNOLOGY**

**Evaluation for Corrosion Resistance of Nano-Cluster Layer and Biofilm  
Formation**

**Hideyuki Kanematsu<sup>\*1</sup>, Takehiko Hihara<sup>2</sup>, Tomoyuki Ishihara<sup>3</sup>, Kyoki Imura<sup>4</sup>, Takeshi Kogo<sup>5</sup>**

<sup>\*1,5</sup>Department of Materials Science and Engineering, Suzuka National College of Technology (SNCT),  
Shiroko-cho, Mie, 510-0294, Japan

<sup>2</sup>Department of Environmental and Materials Engineering, Nagoya Institute of Technology (NITEC),  
Gokiso-cho, Showa-ku, Nagoya, Aichi 486-8555, Japan

<sup>3</sup>Advanced course student, Dept. Materials Science and Engineering, Suzuka National College of  
Technology (SNCT), Shiroko-cho, Mie, 510-0294, Japan

<sup>4</sup>Graduate Student, Department of Environmental and Materials Engineering, Nagoya Institute of  
Technology (NITEC), Gokiso-cho, Showa-ku, Nagoya, Aichi 486-8555, Japan

[kanemats@mse.suzuka-ct.ac.jp](mailto:kanemats@mse.suzuka-ct.ac.jp)

---

**Abstract**

Biofilm is an inhomogeneous film-like matter which attached bacteria produce on materials surfaces. Recently, the knowledge and information about the interaction between biofilm and metallic materials have been revealed gradually and it has been clarified that biofilm would be involved in many interfacial phenomena on metallic materials, such as corrosion, taint in various ways, antibacterial effects etc. The control for biofilm formation on materials surface would be a key factor for various industrial problems from the viewpoint. In this paper, we focused on nano-particles cluster stacked films or single one of chromium and/or nickel produced by helicon sputtering process. The specimens having those films on their surfaces were immersed by a specially devised biofilm formation apparatus. Then the biofilm formation behaviors for the specimens were observed and evaluated by a 3D visualized microscopy, a low pressure SEM-EDX etc. And the possibility of biofilm control for those nano-particles cluster films and the relation between biofilm and corrosion were discussed.

**Keywords:** Biofilm, microbially influenced corrosion, nano-particles cluster, helicon sputtering, Cr/Ni double layers

---

**Introduction**

The economical loss caused by the corrosion of materials is enormous. In most of the advanced countries, it costs about several percentage of GNP[1]. Particularly the corrosion of marine structures such as ships, bridges in coastal areas are serious. They are caused by the coastal atmosphere including chloride or by the direct contact with wave splash. However, the significant part of the corrosion might be caused by bacteria. It is called microbially influenced corrosion (MIC), generally[1-3]. The mechanism of MIC has been discussed by many researchers so far, even though there are not any established theory at this point. Some researchers suggest the relation and connection of biofilm to MIC[4]. Not only the corrosion in coastal areas, but also the general atmospheric corrosion might be related to biofilm, since the corrosion would be caused by the pre-existence of thin water film. Bacteria exist everywhere and the biofilm could form with water on any material surfaces.

Fig1 shows the general mechanism of biofilm formation on solid materials. In natural environments, metal surfaces form thin water film on them generally. And carbon compounds adsorb on them and form thin film-like matters. It is called the "conditioning film". Then the planktonic bacteria floating in ambient air and water move toward the conditioning film as nutrient and adsorb on the material surface. The attached bacteria excrete polymeric substances such as extracellular polysaccharides (EPS) simultaneously, when the number of attached bacteria exceeds a certain threshold value. At this point, the material surface is covered by biofilm containing more than 85% water, EPS, bacteria and other components entering the biofilm from outside[5-8].

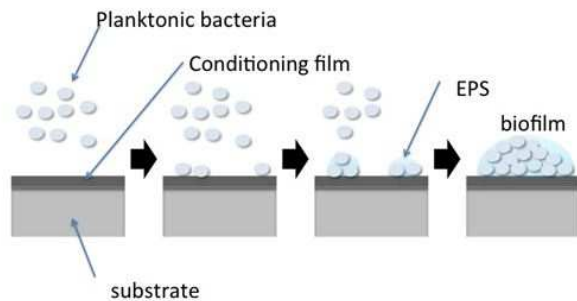


**Fig.1 Biofilm formation process**

Since the corrosion and some other detrimental effects caused by biofilm should be controlled, the biofilm has to be moderated, inhibited or controlled properly. Generally the metallic elements existing on materials surfaces could affect the biofilm formation behavior[9-10]. Particularly, we confirmed that the iron would accelerate biofilm formation and also that the reason could be attributed to the dissolution of iron into aqueous phases[11-13]. Therefore, the dissolution of iron has to be stopped somehow for the biofilm control and we have investigated some coating processes for the purpose so far[14-21].

In this study, we focused on “nano-particles cluster film” composed of chromium, nickel and/or iron. The nano-particles cluster film is defined as film composed of several hundreds of atoms or molecules. The activity is very high and it generally shows some different properties from the bulk material. Therefore, some different unique effects from those in our previous studies relating to the control of biofilm formation were expected. The nano-particles cluster thin films of chromium, nickel and stainless steel components were produced on steels firstly and their biofilm formation behavior was observed when they were immersed in an accelerated biofilm formation reactor.

## Experimental

### Specimens

#### *Helicon sputtering films (HS)*

A carbon steel (JIS SS400) was used as substrate. The surface was polished mechanically by a series of abrasive papers (up to #600). Helicon sputtering apparatus was used to make thin films. The system was evacuated down to  $10^{-4}$ Torr and then a high frequency electric field was applied to a coil in the high vacuum atmosphere to produce Ar plasma. The argon gas ion in the plasma was accelerated and collided against the target to flick the surface atoms and to deposit them on the substrate. Chromium and nickel were used as target separately and the double layers in which chromium layer was the upper were formed. The film

thickness was controlled and adjusted by the sputtering time. And three kinds of specimens from the viewpoint of film thickness were formed. The first one was the 50 nm double layers composed of 25nm nickel film and chromium one, respectively. The second was the 120 nm double layer composed of 60 nm nickel and chromium films, respectively. The final was the 800 nm double layers composed of 400 nm nickel and chromium single layers, respectively. And in addition of those double layer specimens, pure iron and stainless steel (SUS 304) films (Both films' thicknesses were 120 nm.) were also formed by the sputtering process for the reference. In this paper, those films produced by the sputtering process were called helicon sputtering films.

#### *Nano particles cluster film (NPC)*

The carbon steel (JIS SS400) was also used as substrate. The surface was also polished mechanically by a series of abrasive papers (up to #600). A special apparatus was used to produce condensed nano-particles cluster in plasma gases. Firstly, the glow discharge plasma was produced in low vacuum atmosphere. And the produced rare gas ion collided against the target to flick the surface atoms. The sputtered metallic atom was carried with helium gas flow. During the process, metallic atoms collided against rare gas atoms to produce super-saturated situation. And finally, nano-particles cluster was produced and deposited on the substrate set in a special chamber in the system. The average diameter of cluster was approximately 10 nm. The film thickness was also controlled by the sputtering time. And also in this case, three kind of specimens from the viewpoint of film thickness were prepared. The total thicknesses were 50nm, 120nm and 800nm and the constitution was quite the same with those for helicon sputtering films. Pure iron and stainless steel films (JIS SUS 304) were also produced by the process. In this paper, the film was called nano particles cluster film.

#### *Helicon sputtering – nano particles cluster film (HS-NPC)*

Pure iron was used as substrate and the surface was polished mechanically by a series of abrasive papers (up to #600). The apparatuses for helicon sputtering film and nano particles cluster film were used. Stainless steel was used as target and the film was produced on the substrate. The double layer films were composed of helicon sputtering and nano-cluster in which the latter was the upper layer. The thicknesses of both films were 60 nm, respectively and the total thickness was 120 nm. In this paper, the film was called helicon sputtering – nano particles cluster film.

#### *Heat treatments*

Some of the specimens were heat treated in vacuum by an infrared heating furnace (Thermo Riko Co.). The specimens were heated at the rate of 20

degrees per minute up to 400 degrees Celsius. They were maintained at the temperature for 30 minutes and cooled down gradually to the room temperature in about

20 minutes. The detailed information was summarized in Table 1 – 3.

**Table 1 Ni-Cr double layers used for CV measurements.**

	specimens	targets	film thickness	heattreatd?
1	carbon steel (substrate)	-	-	no
2	HS	Ni, Cr	Ni:25nm, Cr:25nm	no
3			Ni:60nm, Cr:60nm	yes
4	NPC		Ni:25nm, Cr:25nm	no
5			Ni:60nm, Cr:60nm	no
6				yes

**Table 2 Ni-Cr double layers used for BF measurements.**

	specimens	target	film thickness	heat treated?
1	carbon steel (substrate)	-	-	no
2	HS	Ni, Cr	Ni:400nm, Cr:400nm	no
3				yes
4	NPC			no
5				yes

**Table 3 Stainless steel double layers used for BF measurements.**

	specimens	target	film thickness	heat treated?
1	Pure iron(substrate)	-	-	no
2	HP	SUS304	120nm	
3	NPC			
4	HP-NPC		60nm+60nm	

**Cyclic voltammetry (CV) measurements**

The specimens shown in Table 1 were used for the measurement. The lead wire was attached to the opposite side with an organic adhesive against that of formed films, and the contact points were covered with conductive pastes to ensure the electronic conductivity. All parts of the specimens except for the metallic electrode surfaces were covered with non-conductive pastes. The specimens were immersed into artificial sea water solutions (Daigo artificial sea water, Wako Pure Chemicals Co.) filled in a glass cell. The pH of the solution was about 8. The specimen was set as working

electrode and the platinum plate was used as counter electrode. Silver/Silver Chloride electrode in 3.3mol KCl solution was used as reference electrode. All of these three electrodes were connected to a potentiostat (Hokuto Denko Co.). With a function generator (Hokuto Denko Co.), the potential was scanned anodically after 30 minutes immersion, until the anodic current reached 1.0mA or the potential reached 0V. Then it was scanned anodically until the potential reached -1.0V. The scan rate was 10mV/sec. The output potential and current were recorded by a recorder (Hioki Co.) and the results

were analyzed to evaluate the corrosion resistance in sea water.

### Biofilm Formation (BF) measurements

We devised a biofilm reactor where biofilm formation could occur artificially and reproducibly on the laboratory scale. Fig.2 shows the apparatus. A transparent acryl column (external diameter: 50mm; inside diameter: 40mm, the entire length: 440mm) was prepared. In the column, the long support over the entire length of column was inserted, so that its several artificial projection portions could fix specimens by screws and holes. Both ends of the column have the flange parts whose diameters were 110mm. They made pipes from/to the circulation system contact closely to the column and basically constituted the system. The bottom tank was filled with clean water and the water was circulated through the system by the pump at about the flow rate of 6L/min. At a part of the circulation system, after the water flows out of the column, and just above the bottom tank, water was designed to pour onto the patterned intended surface of a plate. The shape of the plate was 0.1 x 0.2 m and the surface was patterned to increase the surface area. On the plate, the germ in the ambient air were mixed with water. The air was blown onto the plate also by the fan set just above the plate. And as a result, the number of bacteria in the water was increased in the circulated water. The experiment to form biofilm on the specimens continued in about several weeks at maximum. And after the exposure, the specimen was taken out from the system and served for various observation and measurements.

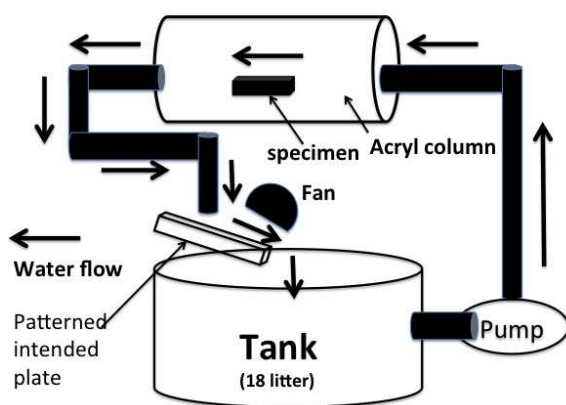


Fig.2 An apparatus for biofilm formation from germs in air.

### Surface Analyses

Some surface analyses were carried out by various surface measurement apparatuses. One of them is a scanning electron microscope with an EDX function (TM 1000, Hitachi Co.). It is generally very hard for the

usual SEM to observe biofilm properly, since high vacuum atmosphere available for the apparatus, since it would break biofilm structure down to pretty much extent. However, the SEM used in this experiment was operative under low vacuum pressures and it could be applied to biofilm observation. Using the low vacuum SEM-EDX, we could observe the morphology of biofilm and analyze elements in it.

The second apparatus was a 3D optical microscope (VW-9000, Keyence Co.). The apparatus enabled us to take usual magnified optical microscopic pictures as usual. In addition, the 3D morphological images could be taken, when images obtained by moving the specimens on the stage slightly were superimposed.

## Results and Discussions

### Cyclic Voltammetry (CV)

Potential-current curves (cyclic voltammograms) obtained by the cyclic voltammetry were shown in Fig.3. Fig.3(a) is the figure for the comparison between the corrosion resistances of 120 nm NPC with heat treatment and without heat treatment. When the result is compared with those for HS specimens, one could see generally that the current was generally high, regardless of heat treatments. And the figure also shows that the current repeated to vibrate slightly in a relatively wide potential range. This could be attributed to that the passivation film formed on the specimen was unstable and repeated to form and break, and it also suggests that the corrosion resistance decreased due to it. NPC did not cover so many parts of the surfaces, being compared with HS specimens. Therefore, the iron substrate covered with films became exposed partly. When the heat treatment was applied, the surface diffusion occurred, nano-cluster particles clumped together, caused a massive expansion and covered wider areas of the specimen's surface. And the alloying by the heat treatment improved the corrosion resistance at the same time.

Fig.3(b) shows the results for the comparison between the corrosion resistances of 50nm HS and NPC. At the potentials around the initiation of pitting corrosion (pitting potential), the slope of increasing current for NPC was steeper than that for HS. It indicates that the NPC's corrosion rate was larger than that for HS. The reason could be attributed also to that the coverage for NPC was lower than that for HS.

Fig.3 (c) shows the comparison between the corrosion resistance of HP and NPC films with the heat treatment. Since the slope of increasing current at around the pitting potential for NPC was larger than that for HS, we could confirm also in this case that NPC was easier to corrode than HS.

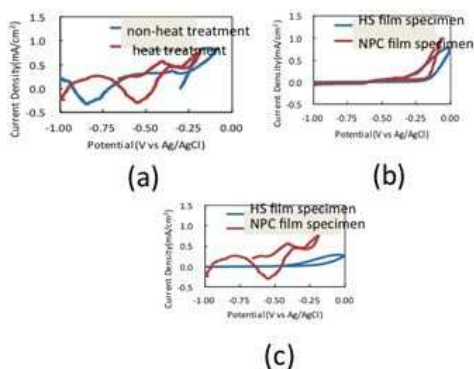


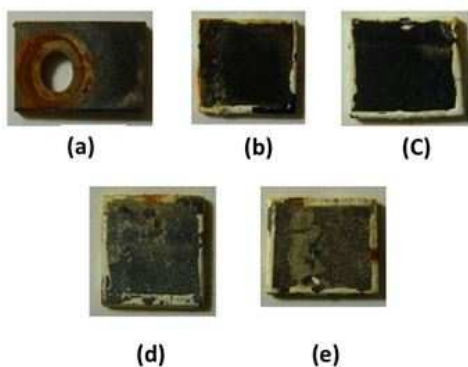
**Fig.3** Cyclic voltammograms for various specimens (a) NPC with or without heat treatments. (b) HS and NPC without heat treatment, (c) HS and NPC with heat treatment.

**Biofilm Formation (BF)**

Fig.4 shows the appearance of Cr/Ni double layers. Regarding the carbon steel as substrate and also NPC, the immersion period was one week, while that was 17 days for HS.

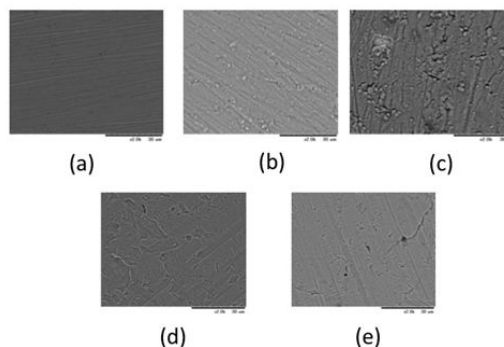
Fig.4(a) indicates that there were lots of pits and corrosion products on the surface of carbon steel. Fig.4(b) and Fig.4(c) indicate that there were fewer pits and corrosion products on NPC surface than on the substrate. On the other hand, there were almost no pits/corrosion products on HS. It also suggests that HS had higher corrosion resistance than NPC due to the higher coverage.

Fig.4(d) and Fig.4(e) shows white corrosion products on the entire of surface. However, any remarkable pits and corrosion products were not observed and it can be concluded that the substrate iron was protected almost completely.



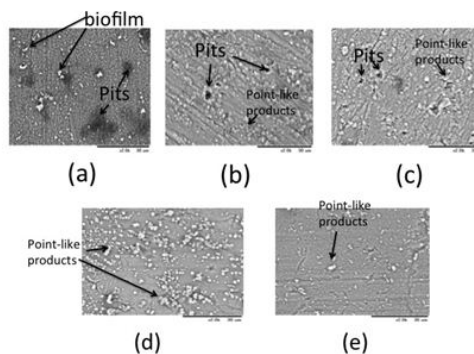
**Fig.4** Appearances of various specimens after BF tests. (a) Carbon steel (b) NPC without heat treatment (c) NPC with heat treatment (d) HS without heat treatment (e) HS with heat treatment, (a),(b) and (c): test period was one week. (d) and (e): test period was 17 days.

Fig.5 shows the SEM photos of Cr/Ni double layer specimens taken before the immersion tests. In Fig.5(b) and Fig.5(c), the remarkable concavo-convex surface profiles were recognized, regardless of the heat treatment. According to Fig.5(a), (d) and (e), the less level surfaces were observed for the substrate and HS.



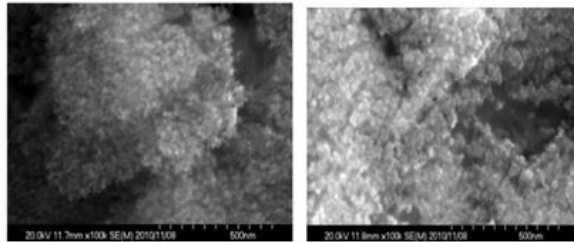
**Fig.5** SEM photos before BF tests. (a) carbon steel (b) NPC without heat treatment (c) NPC with heat treatment (d) HS without heat treatment (e) HS with heat treatment

Fig.6 shows the SEM photos for various Cr/Ni double layer specimens after the immersion into the biofilm formation reactors. As shown in Fig.6(a), lots of pits were produced on the surface of the carbon steel substrate and in addition to them, biofilm was observed on the whole surface. Also in Fig.6(b) and Fig.6(c) for NPC, pits were observed on the surfaces and the odd-shaped surface became remarkable after the immersion. As shown in Fig.6(d) and Fig.6(e), point-like products whose diameters were 2 micro meters were observed on the surfaces of HS specimens. There were more point-like products for HS specimens without heat treatments than for that with heat treatment. Therefore we presumed that the heat treatment could control the formation of products. The point-like products tended to be observed more at uneven areas.



**Fig.6 SEM photos after BF tests. (a) carbon steel (b) NPC without heat treatment (c) NPC with heat treatment (d) HS without heat treatment (e) HS with heat treatment**

Fig.7 (a) shows the SEM photo for NPC without heat treatment. The photo suggests that the nano-particles cluster was very fine and it coincides with the statement that the diameter was approximately 5 nm. Fig.7(b) shows the SEM photo for NPC with heat treatment. It suggests that the heat treatment promoted the diffusion and aggregation [22].



(a) (b)

**Fig.7 Aggregation of nano-particles cluster by heat treatments observed by SEM. (a) before heat treatment (b) after heat treatments**

Using the EDX function, we analyzed elements on the surfaces of substrate and Cr/Ni double layer specimens. Each surface area was 0.32mm<sup>2</sup>. The measured concentrations of nickel, iron and silicon were shown in Fig.8. Fig.8(a) and Fig.8(b) show that nickel and iron were measured not for HS, but for NPC. It suggests that the under nickel layer and iron substrate became remarkable, since NPC's coverage over the substrate and the under layer was relatively low. Being compared with the result for heat treated NPC, the non-heat treated NPC showed higher concentration of nickel and iron under the upper chromium layers. It suggests that the heat treatment of NPC promoted the covering through diffusion on the surface whose coverage was originally insufficient.=

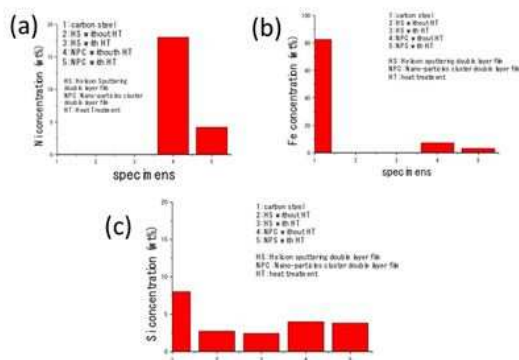
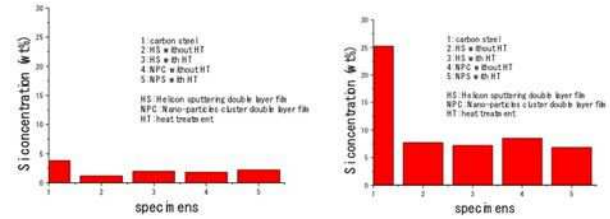


**Fig.8 Ni, Fe and Si concentrations for various specimens. (a) Ni (b) Fe (c) Si**

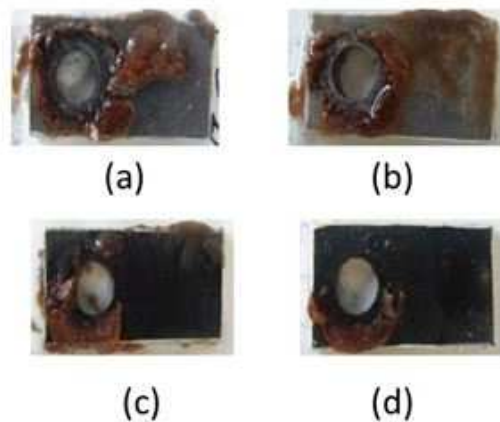
Generally Biofilm is composed of water, exopolymeric substances (EPS) and microbes and it incorporates silicon components from water outside [23]. However in this case, any specimens did not contain silicon. Therefore, silicon contents could be considered the signal for biofilm formation. The silicon contents should have increased with the biofilm growth. From the standpoint, the carbon steel as substrate was the highest to form biofilm on its surface, followed by NPC and HS in this order.



(a) (b)

**Fig.9 Si concentrations for various areas on each specimen. (a) less corrosive part (b) on a point-like product**

We analyzed point analyses of EDX both on the point-like products and also the parts of surfaces for the carbon steel and Cr/Ni double layers where corrosion products were not observed. The silicon contents on those parts were shown in Fig.9. The comparison between Fig.9(a) and Fig.9(b) made clear that silicon contents on the point-like products were higher than on the non-corrosion parts. Therefore, the point-like products could be related to biofilm formation and growth. When we come to think about the high density of point-like products at uneven parts, we can presume that biofilm is easy to form at uneven and inhomogeneous parts.



(a) (b) (c) (d)

**Fig.10 Appearances of various specimens after BF tests. (a) pure iron (b) HS (c) NPC (d) HS-NPC**

We carried out the exposure test in the biofilm reactor also for pure iron and stainless steel film specimens. The appearance was shown in Fig.10. The circular holes in the figures was made inevitably to fix the specimens in the column with flowing water of the biofilm reactor. Since they were crevices, the brown corrosion products (iron oxides mainly) were seen around the holes. However, white films covered the other parts of surfaces, even though the photos could not reflect the color and the brightness properly due to inappropriate light angles and the films looked blackish actually. The white films covered pure iron specimen the most, as shown in Fig.10(a). Regarding HS, NPC and HS-NPC specimens, the coverage looked almost the same.

We carried out the exposure test in the biofilm reactor also for pure iron and stainless steel film specimens. The appearance was shown in Fig.10. The circular holes in the figures was made inevitably to fix the specimens in the column with flowing water of the biofilm reactor. Since they were crevices, the brown corrosion products (iron oxides mainly) were seen around the holes. However, white films covered the other parts of surfaces, even though the photos could not reflect the color and the brightness properly due to inappropriate light angles and the films looked blackish actually. The white films covered pure iron specimen the most, as shown in Fig.10(a). Regarding HS, NPC and HS-NPC specimens, the coverage looked almost the same.

The SEM photos for the same specimens after the exposure tests were shown in Fig.11. As shown in Fig.11(a), there were lots of corrosion products on the surface of pure iron specimen. At the same time, pitting and micro-algae related to biofilm formation could be well observed. As shown in Fig.11(b), those were not so observed for HS specimen. For NPC, pitting was the most remarkable. Fig.11 (d) showed that corrosion did not occur for HS-NPC specimen. The results for elemental analysis by EDX for pure iron and stainless steel film specimen were shown in Fig.12. The figure shows silicon contents for various specimens. As shown in Fig.12, the silicon content for pure iron specimen was the highest (8.6%), followed by HPC (3.4%), HS (3.1%), and HS-NPC (2.1%) in this order. All of specimens' surfaces contained silicon contents to some extent after the BF tests, while those before the tests didn't show any significant silicon contents. It suggests that all of specimens formed biofilm in varying degrees. From the viewpoint of biofilm formation and growth followed by microbial corrosion, the pure iron specimen would be the most vulnerable to corrosion, being followed by NPC, HS and HS-NPC in this order.

Fig.13 shows 3D images for the surfaces of pure iron and stainless steels specimens after BF tests. The series of photos in the left sides of Fig.13 correspond to the plain views and those in the right side to virtual 3D images from an angle. As shown in the color bars in the latters, the higher area was described in red, while the lower in blue. And the color between red and blue was changed gradually, depending on the change of height. The tower-like matters in these figures were biofilm.

Once corrosion occurs, the metallic materials surfaces are generally lost. At the same time, biofilm formed on the surfaces is almost removed together to some extent. On the other hand, biofilm formation is produced by the attachment of bacteria on materials surfaces which could be attracted by iron dissolution. Therefore, the biofilm growth as a result should be considered a balance between corrosion dissolution of iron substrate and biofilm formation and growth rate. From the standpoint, the results shown in Fig.13 could be explained as follows.

As shown in Fig.13(a), the pure iron specimen corroded significantly and the formed biofilm disappeared almost completely. Therefore, there were few biofilm on the surface, while the corrosion traits and holes were observed. Fig.13(b) shows the result for HS film specimen. Since the substrate surface was covered by stainless steel films, the iron dissolution was controlled and as a result, the biofilm formation was also controlled to some extent. Fig.13(c) shows the result for NPC. Since the substrate iron was coated by stainless steel film, the iron dissolution was controlled more than the pure iron specimen. However, the specimen corroded to some extent, since the coverage was not enough and the iron substrate appeared and had direct contacts for some parts of the surface. As a result, the 3D image was the mixture of corrosion traits and biofilm. Fig.13 (d) corresponds to the result of HS-NPC film specimen. There were almost no corrosion traits and the patterned uneven surface was only composed of biofilm mainly. However, the biofilm formation was also well controlled, being compared with other specimens.

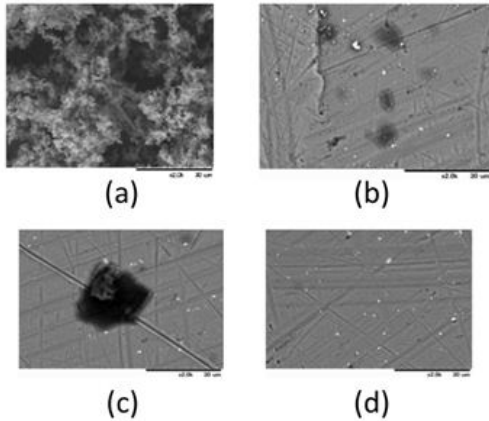


Fig.11 SEM photos for various specimens after BF tests. (a) pure iron (b) HS (c) NPC (d) HS-NPC

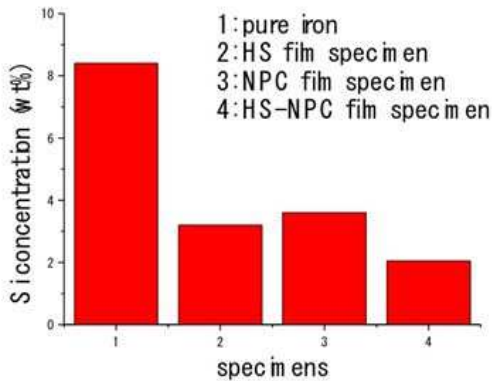


Fig.12 Si concentrations for pure iron and various stainless film specimens.

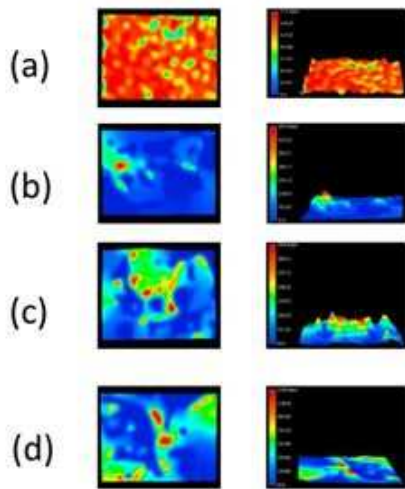


Fig.13 3D images by the optical microscopy for various specimens. (a) pure iron (b) HS (c) NPC (d) HS-NPC

### Conclusions

In this paper, various Cr-Ni-Fe films were prepared by helicon-sputtering, plasma gas condensation method (for nano-particles cluster formation) etc. and their biofilm formation and the corrosion characteristics were investigated by cyclic voltammetry, biofilm formation tests and surface analyses by SEM-EDX or 3D images optical microscopy. And as a result, the following points were obtained.

- (1) NPC film specimens generally corroded the most. The corrosion resistance was improved by a heat treatment, since it promoted the aggregation of nano-particles clusters and increased the surface coverage as a result.
- (2) The corrosion resistance for HS film specimens were generally higher than that for NPC film specimens.
- (3) When NPC was layered on HS layer, the crevices of HS were filled with NPC and the corrosion resistance was improved drastically.

### Acknowledgment

This study was supported financially by NEDO (New Energy and Industrial Technology Development Organization) as a part of the project entitled "The development of minimum life cycle cost heliostat by the utilization of biotechnology and anti-fogged glass". And we appreciate Hikari Kikai Co. for their kind cooperation very highly.

### References

- [1] Flemming, H.-C., Murthy, S.P., Venkatesan, R., and Cooksey, K.E., Marine and Industrial Biofouling, Springer 2009
- [2] Heitz, E., Flemming, H.-C., and Sand, W., Microbially influenced corrosion of materials: scientific and engineering aspects 1996, Berlin; New York: Springer-Verlag. xiv, 475 p.
- [3] Little, B. and Lee, J., Microbiologically influenced corrosion 2007: Wiley.
- [4] Hamilton, W.A., Microbial Biofilms, in Microbial Biofilms, H.M. Lappin-Scott and J.W. Costerton, Editors. 1995, Cambridge University Press: Cambridge University Press. p. 178.
- [5] Costerton, J.W., Stewart, P.S., and Greenberg, E.P., Bacterial biofilms: "From the natural environment to infectious diseases". Nature Reviews Microbiology, 284.284: p. 1318-1322.
- [6] Characklis, W.G. and Marshall, K.C., Biofilms, ed. W.G. Characklis and K.C. Marshall, New York: John Wiley & Sons, Inc. 1990



- [7] Costerton, J.W. and Lappin-Scott, H.M., Introduction to Microbial Biofilms, in *Microbial Biofilms*, H.M. Lappin-Scott and J.W. Costerton, Editors. 1995, Cambridge University Press. p. 1-11.
- [8] Costerton, J.W., Introduction to biofilm. *International Journal of Antimicrobial Agents.*, 1999. 11: p. 217-221; discussion 237-239.
- [9] Kanematsu, H., Ikigai, H., and Yoshitake, M., Antibacterial Eco-plating Based on HACCP and Biofilm. *Bulletin of the Iron and Steel Institute of Japan*, 2008.13(1): p. 27-34.
- [10] Kanematsu, H., Ikigai, H., and Yoshitake, M., Evaluation of Various Metallic Coatings on Steel to Mitigate Biofilm Formation. *International Journal of Molecular Science*, 2009.10(2): p. 559-571.
- [11] Kanematsu, H., Ikegai, H., and Kuroda, D., Biofilm and Metallic Materials. *Rust Prevention and Control, Japan*, 2011.55(10): p. 369-377.
- [12] Ikigai, H., Kanematsu, H., and Kuroda, D., Control of microbial growth by metallic materials. *Journal of the Japan Institute of Light Metals*, 2011.61(4): p. 160-166.
- [13] Kanematsu, H., Ikigai, H., and Kuroda, D., Microbiofouling on Metallic Surfaces and Various Engineering Problems as a Result. *Journal of High Temperature Society of Japan*, 2011.37(1): p. 17-24.
- [14] Kanematsu, H., Kougo, T., Kuroda, D., Itoh, H., and Noorani, R., Prevention Coating Against Biofilm Formation, in *Sur/Fin Asia-Pacific 2012*, S. Hemsley, Editor 2012, Singapore Surface Engineering Association: Singapore. p. 52-56.
- [15] Kanematsu, H., kuroda, D., Chika, O., Murakami, K., and Yokoyama, S., Biofouling on Spray Coated Concretes in Marine Environment, in *The 16th International Congress on Marine Corrosion and Fouling 2012*: Seattle, Washington, the USA. p. 72.
- [16] Kanematsu, H., Kuroda, D., Itoh, H., and Ikigai, H., Biofilm Formation of a Closed Loop System And Its Visualization. *CAMP-ISIJ*, 2012.25: p. 753-754.
- [17] Kanematsu, H., Kuroda, D., Itoh, H., Kobayashi, T., Noorani, R., Yamamoto, M., and Tsukuda, I., Chemical Surface Treatment for Prevention Against Biofilm Formation, in *Sur/Fin Asia-Pacific 2012*, S. Hemsley, Editor 2012, Singapore Surface Engineering Association: Singapore. p. 57-62.
- [18] Kanematsu, H., Kuroda, D., Kirihara, S., and Itoh, H., The Application of Spray Coating to Anti-fouling and Pro-fouling Surface Treatments for Various Materials, in *4th Asian Conference on Molten Salt Chemistry and Technology*, and *44th Symposium on Molten Salt Chemistry*, Japan2012, Molten Salt Committee, The electrochemical Society of Japan: Hotel Taikanso, Matsushima, Japan. p. 161-167.
- [19] Kanematsu, H., Kuroda, D., Koya, S., and Itoh, H., Development of Production Process on Labo Scale for Biofilm Formation by Immersion into Closed Circulation Water System. *HyoumenGijutsu (Journal of Surface Finishing Society of Japan)*, 2012. 63(7): p. 459-461.
- [20] Kanematsu, H., Kogo, T., Kuroda, D., Itoh, H., and Kirihara, S., Biofilm Formation and Evaluation for Spray Coated Metal Films on Laboratory Scale, in *Thermal Spray 2013 - Innovative Coating Solutions for the Global Economy 2013*, ASM International: Busan, Republic of Korea. p. 520-525.
- [21] Kanematsu, H., Kougo, T., Kuroda, D., Ogino, Y., and Yamamoto, Y., Biofilm Formation Derived from Ambient Air and the Characteristics of Apparatus. *Journal of Physics: Conference Series*, 2013. 433: p. 012031: 1-6.
- [22] TsuyokiImura: Dissertation for bachelor degree, Environmental and Materials Engineering, Nagoya Institute of Technology, 2010.
- [23] Kuroda, D., Kamakura, N., Ito, H., Ikegai, H., and Kanematsu, H., Adhesion of Microorganisms on the Surfaces of Various Metallic Materials Immersed in a Cooling Water Tank of the Package Type Cooling Tower. *Tetsu-to-Hagané*, 2012.98(4): p. 109-116.